Received: 2 June 2023 | Accepted: 19 September 2023

DOI: 10.1002/pros.24632

ORIGINAL ARTICLE

The Prostate WILEY

Berbamine targets cancer stem cells and reverses cabazitaxel resistance via inhibiting IGF2BP1 and p-STAT3 in prostate cancer

Lili Wang PhD[1] | Chen Lyu MSc[1] | Birgit Stadlbauer[1,2] | Alexander Buchner[1,2] | Elfriede Nößner[3] | Heike Pohla[1,2]

[1]Tumor Immunology Laboratory, LIFE Center, LMU Klinikum, University Munich, Munich, Germany

[2]Department of Urology, LMU Klinikum, University Munich, Munich, Germany

[3]Immunoanalytics: Research Group Tissue Control of Immunocytes, Deutsches Forschungszentrum für Gesundheit und Umwelt, Helmholtz Zentrum München, Munich, Germany

Correspondence
Heike Pohla, Tumor Immunology Laboratory, LIFE Center, LMU Klinikum der Universität München, University Munich, Fraunhoferstr 20, Planegg, Munich 82152, Germany.
Email: heike.pohla@med.uni-muenchen.de

Funding information
China Scholarship Council, Grant/Award Number: 201706270196

Abstract

Background: Cancer stem cells (CSCs) are a small subpopulation of tumor cells with the capability of self-renewal and drug resistance, leading to tumor progression and disease relapse. Our study aimed to investigate the antitumor effect of berbamine, extracted from berberis amurensis, on prostate CSCs.

Methods: Sphere formation was used to collect prostate CSCs. The viability, proliferation, invasion, migration, and apoptosis assays were used to evaluate the antitumor effect of berbamine on prostate CSCs. Prostate CSC markers were analyzed by flow cytometry and qRT-PCR. Small RNA sequencing analysis was conducted to analyse miRNAs. Exosomes were extracted using the ExoQuick-TC kit and verified by testing exosomal markers using western blot.

Results: Berbamine targets prostate CSCs. Additionally, berbamine enhanced the antitumor effect of cabazitaxel, a second-line chemotherapeutic drug for advanced prostate cancer, and re-sensitized Cabazitaxel-resistant PCa cells (CabaR-DU145) to cabazitaxel by inhibiting ABCG2, CXCR4, IGF2BP1, and p-STAT3. Berbamine enhanced the expression of let-7 miRNA family and miR-26b and influenced the downstream targets IGF2BP1 and p-STAT3, respectively. Silencing CXCR4 and ABCG2 downregulated the expression of IGF2BP1 and p-STAT3, respectively. Importantly, berbamine enhanced also levels of exosomal let-7 family and miR-26b, suggesting that berbamine possibly influences the expression of let-7 family and miR-26b through exosome delivery. Exosomes derived from berbamine-treated CabaR-DU145 cells re-sensitized the cells to cabazitaxel.

Conclusion: Berbamine enhanced the toxic activity of cabazitaxel and reversed cabazitaxel resistance potentially through CXCR4/exosomal let-7/IGF2BP1 and ABCG2/exosomal miR-26b/p-STAT3 axes.

KEYWORDS
berbamine, cabazitaxel resistance, exosomes, prostate cancer stem cells

1 | INTRODUCTION

Prostate cancer (PCa) is the second most common malignant disease and the fifth leading cause of cancer death among males worldwide in 2020. The incidence of prostate cancer ranks first among men in developed countries. There were 1.4 million new cases of PCa and 375,000 associated deaths worldwide in 2020.[1] Localized PCa patients have a long-term survival period after surgery and radiotherapy. PCa patients at late-stage receiving hormonal treatment show beneficial effects, initially. However, as the disease progresses, most of the patients become resistant to the hormonal therapy reaching the castration-resistant stage of disease (Castration-resistant prostate cancer [CRPC]).[2] Once CRPC developed, patients show a poor survival with 16–18 months from the beginning of progression.[3] At this time, patients will receive chemotherapy, including docetaxel, or cabazitaxel, or a chemotherapy combined with other androgen-modulating agents like abiraterone or enzalutamide.[4] However, most patients develop resistance to those agents, leaving only few therapeutic options.[5,6]

In recent years, increasing studies have focused on cancer stem cells (CSCs), which are a small subpopulation of undifferentiated tumor cells reported to have the capacity of self-renewal, driving tumor progression, and resistance to therapies.[7,8] Several mechanisms associated with therapeutic resistance of CSCs have been revealed, such as cell cycle quiescence,[9] overexpression of efflux pumps,[10] and antiapoptotic proteins,[11] forming a protective niche and repair DNA damage.[12] CSCs can be identified by expressing typical stem cell markers or multidrug resistance markers such as ALDH (aldehyde dehydrogenase), ABCG2 (ATP Binding Cassette Subfamily G Member 2), and the chemokine receptor CXCR4. Researchers also found that prostate cancer stem cell markers can drive progression, therapeutic resistance, and bone metastasis.[13] ABCG2, a member of the ABC transporter family, is often highly expressed in CSCs and can drive CSCs resistance to multiple drugs including taxanes, tyrosine kinase inhibitors, topoisomerase inhibitors, and antimetabolites.[13] It serves as efflux pump to export the antitumor agents from the cancer cells and to maintain low drug concentration.[14] C-X-C Motif Chemokine Receptor 4 (CXCR4) is another marker discussed as prostate cancer stem cell marker. High expression of CXCR4 is associated with an increased risk of distant metastasis and local recurrence in PCa.[15] Repression of CXCR4 resensitizes prostate cancer cells to docetaxel.[16] ALDH1 is an intracellular cancer stem cell marker, which is also related to recurrence and therapeutic resistance in PCa.[17,18]

Berbamine is a natural compound derived from the root of Berberis amurensis. Studies have shown that berbamine has antitumor activities in several types of cancers, such as chronic myeloid leukemia,[19] breast cancer,[20] and melanoma.[21] Promisingly, berbamine can target CSCs in glioblastoma.[22] Cabazitaxel is a second-line therapeutic agent used after docetaxel resistance developed in CRPC patients.[23] Once CRPC patients are resistant to cabazitaxel, treatment options are limited. Therefore, there is a clear medical need to find new agents to inhibit prostate CSCs and to reverse cabazitaxel resistance.

In this study, the antitumor effects of berbamine on prostate CSCs and cabazitaxel-resistant PCa cells were analyzed. The results show that berbamine improves the antitumor effect of cabazitaxel and reverses the cabazitaxel resistance. This indicates that a combination of berbamine and cabazitaxel could be a new treatment option for CRPC patients.

2 | MATERIALS AND METHODS

2.1 | Cell lines and cell culture

The prostate cancer cell lines DU145 and PC-3 were bought from the DSMZ German Collection of Microorganisms and Cell Culture GmbH. Cells were cultured in RPMI 1640 medium with 10% fetal calf serum (FCS "Gold Plus," Bio & Sell, GmbH), 2 mM L-glutamine, 1 mM sodium pyruvate, and 1% minimal essential amino acids (Invitrogen, Life Technologies GmbH) at 37°C in a 5% CO_2 atmosphere. CSCs were generated in DMEM/F12 culture medium supplemented with 2% B-27 (Invitrogen), 10 ng/mL human recombinant basic fibroblast growth factor (bFGF, Sigma Aldrich Chemie GmbH), and 10 ng/mL epidermal growth factor (EGF, Sigma Aldrich). The cabazitaxel-resistant DU145 cell line was established by gradually increasing the cabazitaxel concentration from 1 to 6 nM reaching a resistant status.

2.2 | Sphere formation

Sphere formation was performed to generate the spheric prostate CSCs. DU145 and PC-3 cells were harvested using StemPro Accutase® (Life Technologies, Thermo Fisher Scientific), and seeded in 75 cm^2 ultra-low attachment flasks (Corning Costar) in 10 mL CSCs culture medium. After 7 days of incubation, spheric CSCs were harvested and filtered through a 40 μM nylon mesh cell strainer (BD Biosciences). For enrichment of CSCs, the spheres were dissociated for a second round of sphere formation. To maintain the stem cell properties, only the second to third generation of CSCs was used.

2.3 | Cell viability assay

Cell viability was assessed using the CellTiter Blue Cell Viability Assay (Promega) according to the manufacturer's instructions. Generally, cells were seeded in a 96-well plate and treated with berbamine or cabazitaxel (both from Selleckchem). After 24 h or 48 h, the fluorescence was detected at 560(20) nm excitation/590(10) nm emission using the FLUOstar OPTIMA microplate reader (BMG LABTECH) and the OPTIMA software version 2.0. The logit regression model was used to calculate the half-maximal inhibitory concentration (IC50).

2.4 | Cell proliferation assay

Cell proliferation was evaluated using the CellTiter 96® AQueous One Solution Cell Proliferation Assay (Promega GmbH) according to the manufacturer's instructions. The absorbance was read at 490 nm with the Emax precision microplate reader (MWG Biotech).

2.5 | Apoptosis assay

Cells were treated with berbamine, cabazitaxel, or other agents for 5 days. Then the cells were harvested and resuspended in 100 µL Annexin V Binding Buffer, supplemented with 5 µl APC-Annexin V and 5 µL 7-aminoactinomycin D (7-AAD, BD Biosciences), and incubated for 15 min at room temperature. Next, another volume of 100 µL Annexin V Binding Buffer was added. A minimum of 1×10^4 cells was recorded per sample using the FACSCalibur (Becton Dickinson). BD CellQuest software (version 4.0.2) was used for data acquisition, and FlowJo software (version 9.9.5; Tree Star Inc.) was used for data analyses. The Annexin V positive cells were calculated as apoptotic cells.

2.6 | Scratch wound healing assay

The scratch wound healing assay was applied to test the migration ability of cells. The 24-well culture plates with 2-well silicone inserts per well were used to build a cell-free gap of 500 µm (ibidi GmbH). A total of 2.8×10^4 cells were seeded into each culture insert in a volume of 70 µL, incubated at 37°C until a confluent cell monolayer was achieved. Drugs were added after removal of the inserts. Pictures were taken at different time points, 0, 3, 6, 9, 21, 24, and 27 h. The data were analyzed with the web-based Automated Cellular Analysis System (ACAS, MetaVi Labs) using FastTrack AI image analysis algorithms.

2.7 | Invasion assay

The Boyden Chamber system was used to assess the invasion ability of cells. The transwell inserts in 24-well plates (8.0 µm pores; Falcon) were coated with growth factor reduced Matrigel Basement Matrix (Corning) with 30 µg per insert in a volume of 100 µL and incubated overnight at 37°C in 5% CO_2 atmosphere. A total of 3×10^4 cells were seeded in 250 µL serum-free DMEM medium with/without agents onto the Matrigel. DMEM medium of 750 µL with 10% FCS was added in the lower chamber. After 48 h, the Matrigel on the upper surface was wiped with a moistened cotton swab to remove cells that had not migrated. The cells on the lower surface were fixed with 4% paraformaldehyde for 5 min and stained with 1% crystal violet for 1 min. Cells were counted in three fields per insert using Fiji ImageJ software.[24]

2.8 | Measurement of aldehyde dehydrogenase (ALDH)

ALDH was detected using the ALDEFLUOR kit according to the manufacturer's instructions (StemCell Technologies). The ALDH-expressing cells were detected in the green fluorescence FL1 channel (520–540 nm) of the FACSCalibur. N, N-diethylaminobenzaldehyde (DEAB), an ALDH inhibitor (15 µM) was added as a control.

2.9 | Measurement of proteins using flow cytometry

After being treated with berbamine or other agents, cells were collected, fixed, and permeabilized using the Fixation/Permeabilization Solution Kit (BD Cytofix/Cytoperm) according to the manufacturer's instructions. Afterwards, cells were stained with APC-conjugated ABCG2 monoclonal antibody (clone 5D3/CD338, BD Biosciences), PE-conjugated CXCR4 antibody (clone 12G5/CD184, BD Pharmingen), unconjugated mouse monoclonal STAT3 antibody (clone 124H6, Cell Signaling), and unconjugated mouse monoclonal phospho-STAT3 antibody (Try705, clone 3E2, Cell Signaling). The FITC-conjugated goat antimouse secondary antibody (IgG + IgM (H + L), Dianova) was used. LIVE/DEAD Fixable Blue Dead Cell Stain Kit (Life Technologies) was applied to determine the viability and exclude dead cells during analysis. Measurements were done using the LSRII flow cytometer (BD Biosciences), or FACSCalibur. Data were processed using FlowJo software (version 9.9.5).

2.10 | Quantitative real time PCR (qRT-PCR)

RNA was isolated using the RNeasy Mini-Kit (Qiagen) according to the manufacturer's instructions. A total of 1 µg RNA was used for reverse transcription based on the kit instructions (Promega GmbH). The reverse transcription-polymerase chain reaction was performed with FastStart Essential DNA Green Master kit (Roche) and the Light Cycler® 96 (Roche). A volume of 10 µL reaction was set up with 2 µL cDNA template, 1 µL (5 pmol) forward primer, 1 µL (5 pmol) reverse primer, 5 µL FastStart Essential DNA Green Master reagent mix, and 1 µL PCR grade water. For amplification, a procedure with a hot start with 95°C for 10 min, followed by 40 cycles of denaturation at 95°C for 10 s, annealing at 60°C for 10 s, and extension at 72°C for 10 s was used. Then a melting process with 95°C for 10 s, 65°C for 60 s, and 97°C for 1 s was performed. Data were analyzed using the Light Cycler® 96 software (version 1.1) with the $2^{-\Delta\Delta C_t}$ method. The transcription level of *GAPDH* and *ACTB* was used for normalization. Primers were listed in Supporting Information: Table S1.

2.11 | Small RNA sequencing analysis

A total of 36 samples were prepared to analyze the expression of different miRNAs, including the control, berbamine, cabazitaxel, and berbamine plus cabazitaxel group in DU145 cells, CabaR-DU145 cells, and DU145 CSCs with three times repeat. The total RNAs including small RNAs were isolated by miRNeasy Mini Kit, measured by the NanoDrop ND-1000 spectral photometer (Thermo Fisher Scientific). The following steps were done by the company IMGM Laboratories GmbH and described in the Supporting Information.

Venn diagrams were prepared to show the overall number of differentially expressed small RNAs in all pairwise comparisons and their overlaps between the different cell lines (DU145, CabaR-DU145, and DU145 CSCs). Thereby, all differentially expressed small

RNAs were detected in any pairwise comparisons and any of the biological replicates were included.

2.12 | Individual miRCURY LNA miRNA PCR assay

RNAs were extracted using miRNeasy advanced Mini kit (QIAGEN) according to the manufacturer's instructions. A volume of 2 µL template RNA at 5 ng/µL was used for reverse transcription according to the miRCURY LNA RT kit instructions (QIAGEN). For the PCR procedure, the miRCURY LNA miRNA PCR assay was performed with the Light Cycler® 96 (Roche). A volume of 10 µL reaction was prepared with 5 µL 2× miRCURY SYBR Green Master Mix, 1 µL resuspended PCR primer mix, 3 µL cDNA template, and 1 µL RNase-free water. For amplification, a procedure with a hot start with 95°C for 2 min, and a two-step cycling of 45 cycles: 95°C for 10 s, followed by 56°C for 60 s. Data were analyzed using the Light Cycler® 96 software (version 1.1) with the $2^{-\Delta\Delta C_t}$ method. The transcription level of SNORD48 was used as the internal control for miRNAs, and miR-16 was used as the internal control for exosomal miRNAs. The primers for miRCURY LNA miRNAs of let-7a, let-7b, let-7d, let-7f, let-7g, let-7i, miR-98, miR-26a, and miR-26b were designed and synthesized by Qiagen.

2.13 | Protein inhibitors and siRNA technology

The inhibitors of ABCG2, CXCR4, ALDH1A1, IGF2BP1, phospho-STAT3, were used namely Ko143 (Tocris Biosciences, BioTechne GmbH) at 1 µM, WZ811 (Selleckchem) at 5 µM, NCT-501 (Selleckchem) at 5 µM, BTYNB IMP1 Inhibitor (Cayman Chemical) at 2.5 µM, Cryptotanshinone (Selleckchem) at 4.6 µM, respectively. Small interfering RNAs (siRNAs) were also used to silence ABCG2 and CXCR4, which were designed by Ambion (Life Technologies, Thermo Fisher Scientific). Silencer® Select negative control and Silencer® Select GAPDH positive control were also used as controls. The Silencer® Select siRNAs sequences were shown in Supporting Information: Table S2. The lipofectamine RNAiMAX reagent was used for transfection (Invitrogen, Life Technologies, Thermo Fisher Scientific).

2.14 | Micro-RNA mimics and inhibitors

Mimics of let-7a, let-7b, let-7i, miR-26a, miR-26b, and power inhibitors of let-7, miR-26 were purchased from Qiagen. Cell transfection was performed using lipofectamine RNAiMAX reagent as described in the manufacturer's protocol. The miRCURY LNA miRNA Mimics and Power Inhibitors were shown in Supporting Information: Table S3.

2.15 | Bioinformatical analysis

Immunohistochemistry-based protein expression levels of ABCG2, STAT3, and IGF2BP1 in clinical specimens of prostate normal samples and prostate cancer samples were obtained from the Human Protein Atlas database accessed on August 12, 2023 (https://www.proteinatlas.org/).[25]

The UALCAN portal (https://ualcan.path.uab.edu/index.html), a comprehensive and interactive web resource for analyzing cancer OMICS data,[26] allow us to perform protein expression analysis of the TCGA database accessed on August 12, 2023 (Supporting Information: Figure S16).

2.16 | Western blot analysis

Exosomes were extracted using ExoQuick-TC kit (System Biosciences), and lysed in RIPA lysis buffer (Thermo Fisher), plus 10 µL Phosphatase Inhibitor Cocktail 2 (Sigma), 10 µL Phosphatase Inhibitor Cocktail 3 (Sigma), and 10 µL Protease Inhibitor Cocktail (Sigma) for 15 min on ice, followed by centrifugation at 14,000 rpm for 15 min. The protein concentration was determined using Pierce™ BCA Protein Assay Kit (Thermo Fisher) according to the manufacturer's instructions. At least 50 µg protein was separated by running through the Bolt™ Mini Gels (Life Technologies) and transferred to the PVDF membrane (Thermo Fisher) with the Blot™ 2 Dry Blotting System according to the manufacturer's instructions. Afterwards, the PVDF membranes were incubated with the antibodies using the iBind™ Flex Western System (Invitrogen) overnight at 4°C according to the manufacturer's instructions. The primary antibodies for CD9, TSG101, HSP70, and Calnexin (Abcam) were used 1:1000 diluted. The polyclonal Goat anti-Rabbit IgG (HRP, Abcam) was used as secondary antibody 1:1000 diluted. The transferred proteins were detected and visualized with (SuperSignal™ West Pico PLUS Chemiluminescent Substrate, Thermo Fisher).

2.17 | Detection of exosomal microRNAs

The exosomes were extracted using miRCURY® Exosome Cell/Urine/CSF Kit (Qiagen) according to the manufacturer's instructions. Then, the extracted exosomes were directly proceeded to the RNA isolation step using the miRNeasy Micro Kit (Qiagen) according to the manufacturer's instructions to minimize the risk of RNase contamination. Next, the miRCURY LNA RT kit was used for cDNA synthesis, and the individual miRCURY LNA miRNA PCR assay was performed for the PCR procedure as described in Section 2.12.

2.18 | Statistical methods

All experiments were independently performed at least three times. The analyses were carried out using SPSS version 25.0 (IBM). All numerical data were expressed in form of the average of the values (mean), plus the standard deviation (SD). The graphs were generated using the ggpubr package in R software (version 4.0.3). Data from two different groups were compared using the Mann–Whitney *U*

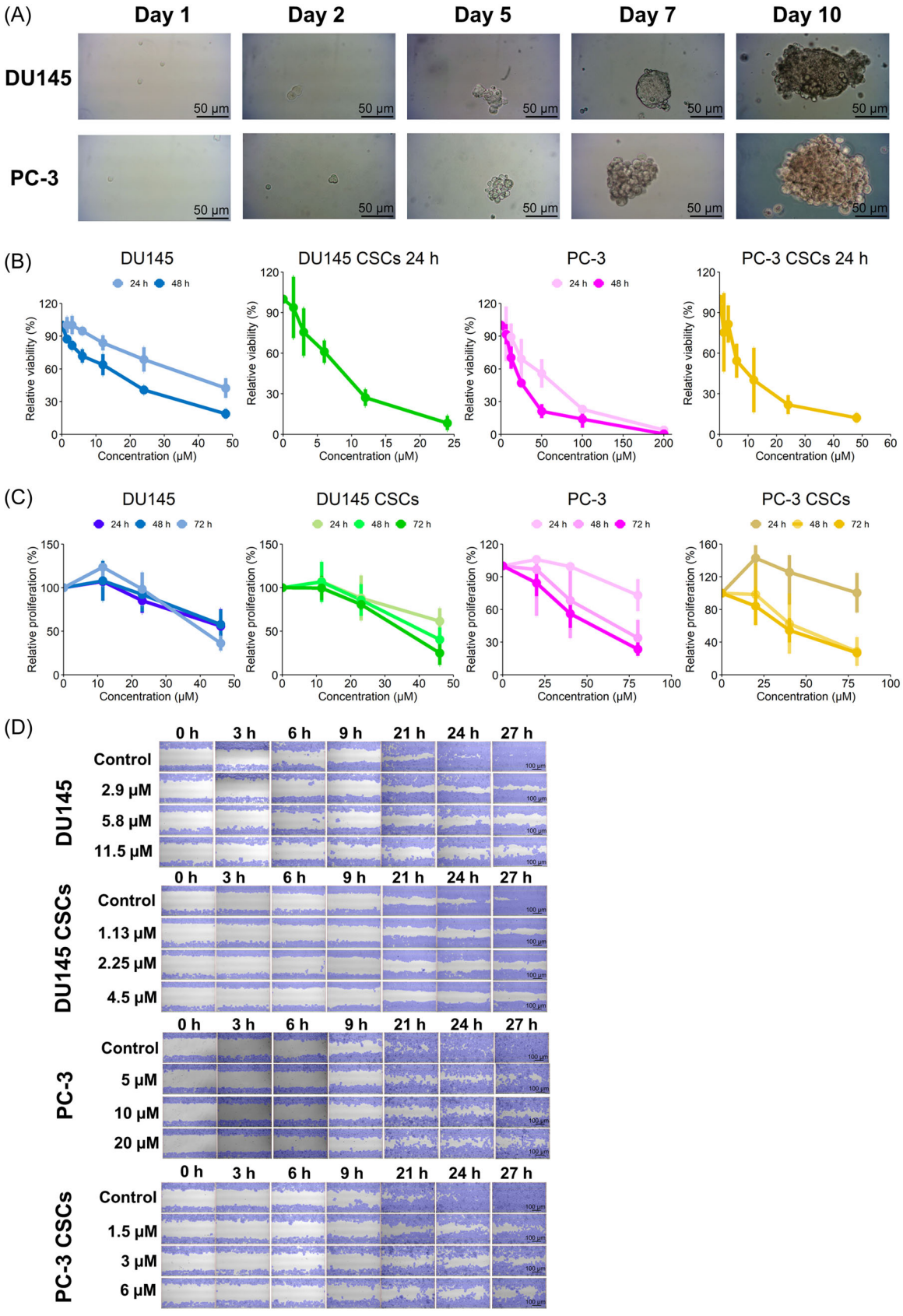

FIGURE 1 (See caption on next page).

test. All p values were two-sided, and $p < 0.05$ was considered significant.

3 | RESULTS

3.1 | Berbamine shows antitumor effects on PCa and PCa stem cells (PCSCs)

Spheric PCSCs were generated using the sphere formation assay as described in Section 2.2. Figure 1A shows the development of spheres within 10 days: PCSCs in the ultra-low attachment flasks with serum-free medium formed nonadherent free-floating spheres, while differentiated adherent prostate cancer cells shrank and died. Those spheres expressed more prostate cancer stem cell markers, including ALDH2, CD44, ALDH1A1, TROP2, ALDH3A1, and ABCG2 than the parental prostate cancer cells, tested in our former study.[27] This study also verified that the spheres expressed more CXCR4 (Figure 3) and EpCAM (Supporting Information: Figure S1), which suggested that those spheres would be PCSCs Then, the PCa cells and PCSCs were treated with different concentrations of berbamine for 24 or 48 h. The CellTiter Blue Cell Viability demonstrated that berbamine inhibited cell viability in a dose-dependent manner (Figure 1B).

The half-maximal inhibitory concentration (IC50) was calculated using the logit regression model by SPSS software as 23 μM for DU145, 9 μM for DU145 CSCs, 40 μM for PC-3, 12 μM for PC-3 CSCs. Results showed that there was no significant difference between spheric DU145 CSCs and adherent DU145 cells (Supporting Information: Figure S2). An inhibitory effect of berbamine on cell proliferation in a dose-dependent manner was also observed using different concentrations of berbamine (0.5 × IC50, IC50, 2 × IC50) for 24, 48, and 72 h (Figure 1C). Results demonstrated spheric PC-3 CSCs were more resistant to berbamine than adherent PC-3 cells during 72 h treatment (Supporting Information: Figure S3). We also evaluated the effect of berbamine on migration and invasion of PCa cells and PCSCs. The scratch wound-healing assay demonstrated that berbamine inhibited the migration of PCa cells and PCSCs as there was less closure of the gap in the presence of the drug (Figure 1D and Supporting Information: S4). The invasion assay showed that the number of invaded cells treated with berbamine decreased significantly for both the adherent cells and stem cells (Figure 1E), which indicated that berbamine could significantly suppress migration and invasion in PCa cells and PCSCs. Cell apoptosis was shown to similar extent in adherent cells and CSCs (Figure 1F and Supporting Information: Figure S5).

3.2 | Berbamine enhances the toxicity of cabazitaxel to PCa and PCSC cells

To investigate if berbamine enhances the antitumor effect of cabazitaxel, we treated cells with both compounds and determined viability, proliferation, invasion, and apoptosis. First, we determined the IC50 of cabazitaxel, which was 3 nM using the method of the logit regression model (Supporting Information: Figure S6). Then, DU145 and DU145 CSCs were treated with 23 μM berbamine combined with different concentrations of cabazitaxel for 48 h. The combination of berbamine and cabazitaxel resulted in a significant decrease in both viability (Figure 2A and Supporting Information: S7) and proliferation (Figure 2B and Supporting Information: S8) of DU145 and DU145 CSCs compared to cabazitaxel alone. Moreover, a significantly higher inhibitory effect of the combination treatment was observed in the invasion assay (Figure 2C). Similarly, the number of apoptotic cells was higher following treatment with cabazitaxel plus berbamine (Figure 2D). A synergistic effect was shown for the combination berbamine and cabazitaxel in the viability assay in DU145 cells calculated by CompuSyn (version 1.0, Supporting Information: Figure S9).

3.3 | Berbamine reverses the cabazitaxel-resistance through inhibiting ABCG2 and CXCR4

Several prostate cancer stem cell markers are responsible for driving drug resistance, and cancer relapse.[13] Therefore, we asked the question if berbamine can influence the expression of these markers.

FIGURE 1 Berbamine shows antitumor effects on PCa cells and stem cells. (A) Sphere formation assay: DU145 cells and PC-3 cells were cultured in serum-free CSC medium for 10 days. The pictures were taken with the microscope camera at ×100 magnification. (B) CellTiter blue assay: berbamine inhibited the viability of DU145 cells, DU145 CSCs, PC-3 cells, and PC-3 CSCs in a dose-dependent manner. (C) CellTiter 96® AQueous One Solution Cell Proliferation Assay: Berbamine inhibited the proliferation of DU145 cells, DU145 CSCs, PC-3, and PC-3 CSCs at the time points of 24, 48, and 72 h in a dose-dependent manner. (D) Scratch wound healing assay: berbamine suppressed migration of DU145 (at 2.9, 5.8, 11.5 μM), DU145 CSCs (at 1.13, 2.25, 4.5 μM), PC-3 (at 5, 10, 20 μM), and PC-3 CSCs (at 1.5, 3, 6 μM). The pictures were captured using a digital microscope camera with ×40 magnification at different time points (0, 3, 6, 9, 21, 24, 27 h). The percentage of covered areas of the gap was calculated by the Automated Cellular Analysis System based on the FastTrack AI image analysis algorithms. (E) Boyden Chamber system for the invasion assay: berbamine inhibited invasion of DU145 cells, DU145 CSCs, PC-3 cells, and PC-3 CSCs at different concentrations (0.5 × IC50, IC50, and 2 × IC50). Pictures were taken from every insert with a digital microscope camera with ×40 magnification for three fields per insert. Cells were counted using the Fiji Image J software, and the cell number in one picture was calculated as invaded cell number. The boxplot shows the number of invaded cells. (F) Apoptosis assay: berbamine induced the apoptosis of DU145 cells and DU145 CSCs. The Annexin-positive cells were considered apoptotic cells. The data were acquired from three different experiments and calculated as means ± SD. $^{*}p < 0.05$, $^{**}p < 0.01$, $^{***}p < 0.001$, $^{****}p < 0.0001$. [Color figure can be viewed at wileyonlinelibrary.com]

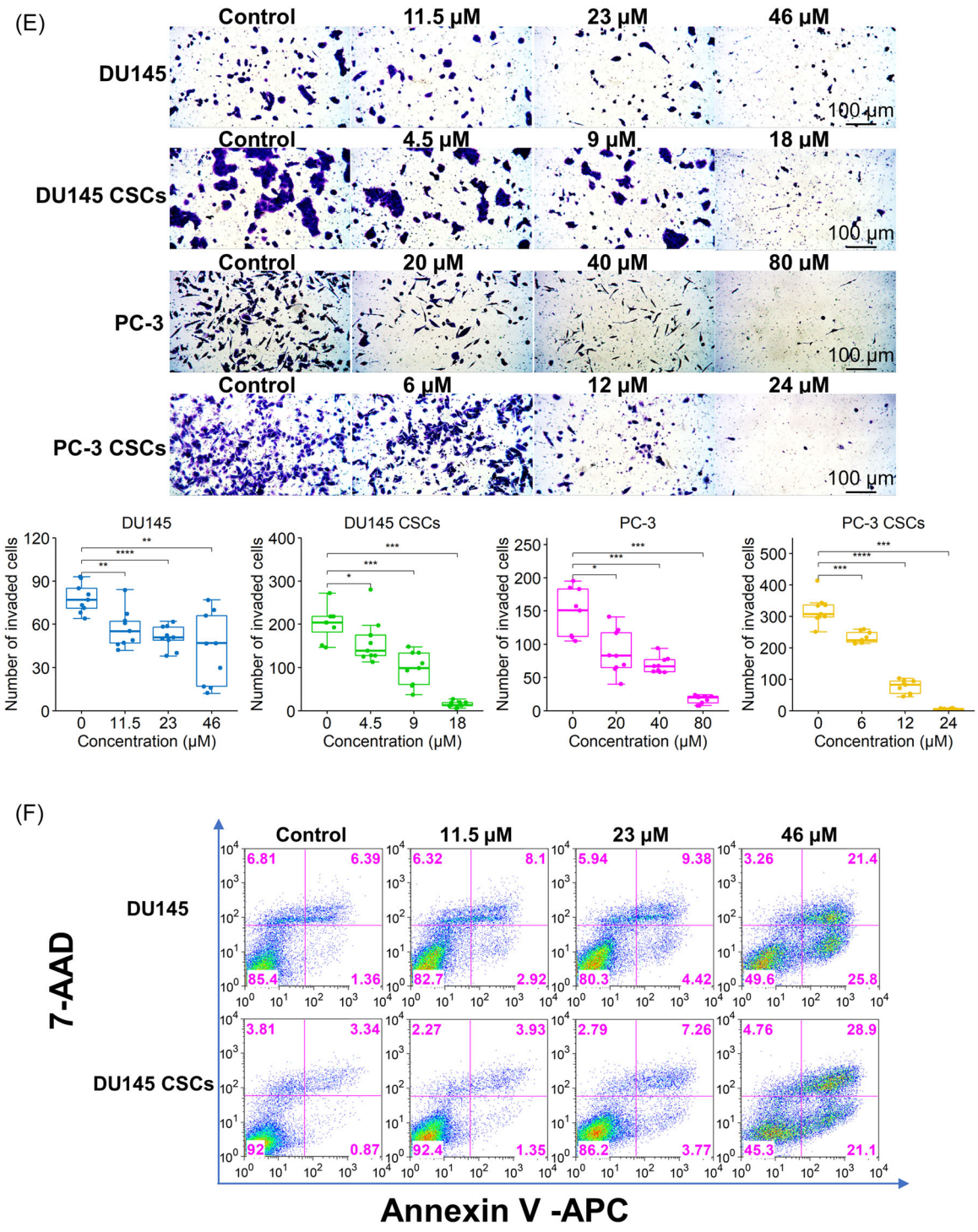

FIGURE 1 (Continued)

Flow cytometry results demonstrated that berbamine inhibited the expression of ALDH, ABCG2, and CXCR4 in DU145-CSCs and PC-3 CSCs (Figure 3A,B, Supporting Information: Figures S10 and S11). Similar results were obtained using qRT-PCR: Berbamine inhibited the expression of *ALDH1A1*, *ABCG2*, and *CXCR4* (Figure 3C and Supporting Information: Figure S12). In a next step, it was explored if suppressing the expression of ALDH1A1, ABCG2, and CXCR4 can sensitize cabazitaxel-resistant DU145 cells to cabazitaxel. Therefore, a cabazitaxel-resistant DU145 cell line (CabaR-DU145) was generated by gradually increasing the dose of cabazitaxel over 8 months (Supporting Information: Figure S13). CabaR-DU145 cells were treated with cabazitaxel at 3 nM combined with the ABCG2 inhibitor Ko143 at 1 μM, or the CXCR4 inhibitor WZ811 at 5 μM, or the ALDH1A1 inhibitors A37 at 10 μM and NCT-501 at 5 μM. Results

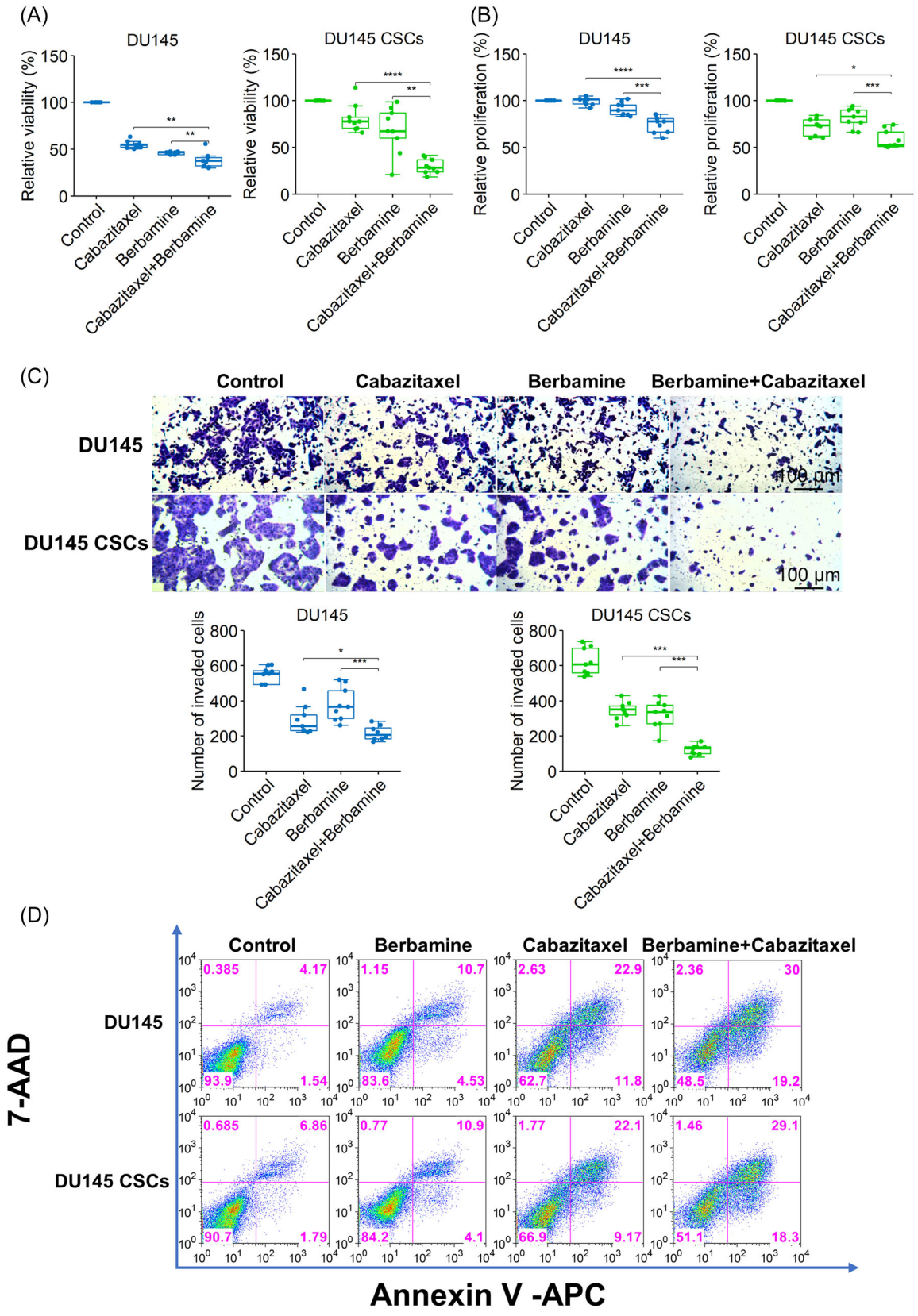

FIGURE 2 Berbamine enhances the toxicity of cabazitaxel to PCa cells and stem cells. (A and B) The combination of berbamine (23 μM) and cabazitaxel (0.75 nM) reduced viability and proliferation of DU145 cells and DU145 CSCs significantly more than each substance alone. (C) Invasion assay: berbamine (23 μM) plus cabazitaxel (1.5 nM) suppressed the invasion of DU145 cells and DU145 CSCs more than cabazitaxel alone. Pictures were captured using the digital microscope camera with ×40 magnification for three fields per insert, and the cell numbers were calculated using the Fiji Image J software. The boxplot shows the number of invaded cells. (D) Apoptosis assay: berbamine plus cabazitaxel induced more apoptotic cells compared to cabazitaxel alone. The Annexin-positive cells were considered as apoptotic cells. The data were acquired from three different experiments and calculated as means ± SD. *$p < 0.05$, **$p < 0.01$, ***$p < 0.001$, ****$p < 0.0001$. [Color figure can be viewed at wileyonlinelibrary.com]

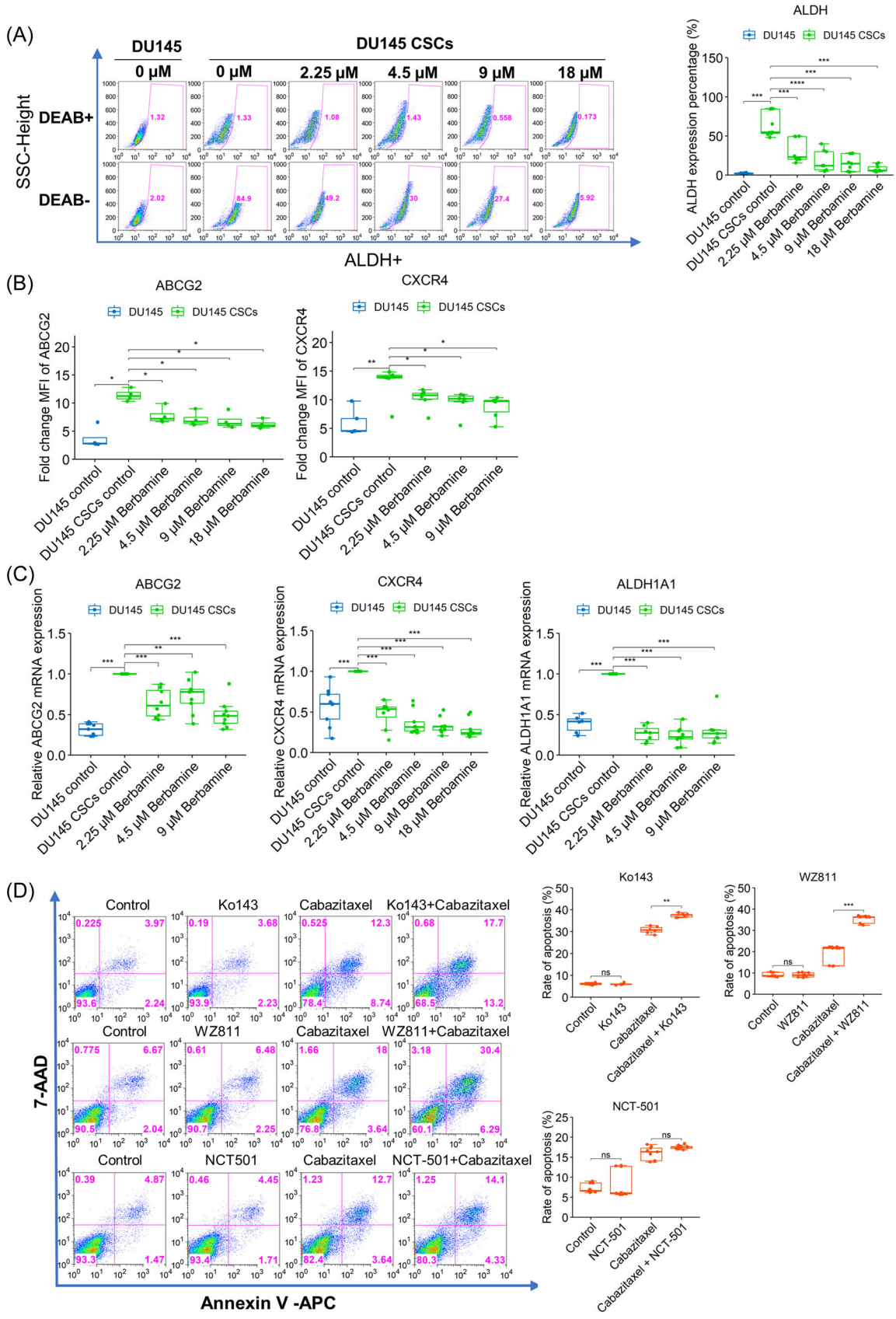

FIGURE 3 (See caption on next page).

showed that inhibition of ABCG2 and CXCR4 increased the apoptosis rate of CabaR-DU145 cells. However, the ALDH1A1 inhibitor (NCT-501) did not influence apoptosis of CabaR-DU145 (Figure 3D). Furthermore, CabaR-DU145 cells expressed more ABCG2 and CXCR4 than the sensitive parental DU145 cells (Supporting Information: Figure S14). These results suggest that berbamine can reverse the cabazitaxel resistance by inhibiting the expression of ABCG2 and CXCR4.

3.4 | Berbamine resensitizes CabaR-DU145 cells to cabazitaxel potentially via CXCR4/let-7/IGF2BP1 and ABCG2/miR-26b/p-STAT3 axes

Small RNA-sequencing was conducted to study the role of microRNAs in the effect of berbamine and the number of small RNAs that were differentially expressed between different treatment conditions and cell types were visualized in Venn diagrams (Supporting Information: Figure S15). The RNA-sequencing results suggested that berbamine enhanced the expression of the members of the let-7 miRNA family, as well as miR-26a, and miR-26b both in CabaR-DU145 cells and DU145 CSCs (Figure 4A). Individual miRCURY LNA miRNA PCR assays verified that berbamine upregulated the expression of the let-7 family members, miR-26a-5p, and miR-26b-5p in CabaR-DU145 cells and DU145 CSCs (Figure 4B,C). The online database of miRDB (http://mirdb.org/mirdb/index.html) was used to investigate downstream targets of the let-7 family members and miR-26, The results revealed several target genes of let-7 family members, including *STARD13* (StAR Related Lipid Transfer Domain Containing 13), *HMGA2* (High-mobility group AT-hook 2, *LIN28B* (lin-28 homolog B), and *IGF2BP1* (Insulin-like growth factor 2 mRNA-binding protein 1) (Table 1).

We observed that berbamine did not influence the expression of *STARD13*, *HMGA2*, or *LIN28B* (data not shown). However, berbamine and mimics of let-7 miRNA family inhibited the expression of *IGF2BP1* (Figure 4D,E), and silencing of *CXCR4* also reduced *IGF2BP1* transcript (Figure 4D), suggesting that berbamine targets PCa stem cells and cabazitaxel-resistant PCa cells through the CXCR4\let-7\IGF2BP1 axis. The observation that the let-7 family targets *IGF2BP1* is consistent with the results of TargetScan (http://www.targetscan.org/vert_72/), which indicated that all members of the let-7 family target the 3′UTR of *IGF2BP1* (Supporting Information: Table S4).

Both berbamine and silencing ABCG2 downregulated the expression of *STAT3* (Signal transducer and activator of transcription 3) on transcriptional level (Figure 4F). More specifically, berbamine and the ABCG2 inhibitor Ko143 decreased phosphorylated-STAT3 (p-STAT3) and upregulated STAT3 expression evidenced by flow cytometry (Figure 4G). Mimics of miR-26b inhibited the expression of p-STAT3, but not STAT3, and inhibitor of miR-26 counteracted the down-regulation of p-STAT3 (Figure 4H). Mimics of miR-26a alone did not decrease the expression of p-STAT3, but in combination with miR-26b mimics p-STAT3 was downregulated (Figure 4H).

Inhibitors of IGF2BP1 (BTYNB IMP1 at 2.5 μM, BTYNB) and p-STAT3 (Cryptotanshinone, at 4.6 μM, CPT) were used to determine if inhibition of IGF2BP1 and p-STAT3 could reverse the cabazitaxel-resistant state. The apoptosis assay showed that both the IGF2BP1 inhibitor and the p-STAT3 inhibitor augmented apoptosis rate compared to cabazitaxel alone (Figure 4I), indicating that the suppression of IGF2BP1 and p-STAT3 reversed the cabazitaxel resistant state.

In conclusion, our results suggested that berbamine targeted both the DU145-CSC and CabaR-DU145 cells through the CXCR4/let-7/IGF2BP1 axis and the ABCG2/miR-26b/p-STAT3 axis.

The expression levels of ABCG2, CXCR4, STAT3, and IGF2BP1 between normal samples and prostate cancer samples were analyzed by the Human Protein Atlas and TCGA database. The results showed that both normal samples and prostate cancer samples highly expressed ABCG2 and STAT3, while low expressed IGF2BP1 on protein level (Supporting Information: Figure S16A). Using the TCGA database normal samples expressed more ABCG2 and STAT3 than prostate cancer samples (Supporting Information: Figure S16B). Taken together, the ABCG2/miR-26b/p-STAT3 axis was of potential clinical significance.

3.5 | Exosomal miRNAs of let-7 family and miR-26b-5p induce apoptosis

To investigate the function of exosomes in the process that berbamine regulated let-7 family and miR-26b, exosomes were isolated from cell culture supernatants using the ExoQuick-TC kit. Exosomes were characterized by exosomal markers (CD9, TSG101, HSP70) in western blot (Figure 5A). Calnexin, which is not found in exosomes, was used as a negative control marker (Supporting Information: Figure S17). To investigate the expression of let-7 and miR-26b in exosomes influenced by berbamine, the miRCURY LNA miRNA PCR assay was performed. Berbamine enhanced the levels of exosomal let-7a, let-7b, let-7i, and miR-26b originating from CabaR-DU145 cells (Figure 5B) AND DU145 CSCs (Figure 5C), which

FIGURE 3 Berbamine reverses the cabazitaxel resistance through inhibiting ABCG2 and CXCR4. (A) ALDEFLUOR assay: berbamine inhibited the expression of ALDH in DU145 CSCs in a dose-dependent manner. The ALDH inhibitor DEAB was used as a control. (B) Flow cytometry: berbamine inhibited the expression of ABCG2 and CXCR4 in DU145 CSCs. DU145 CSCs expressed more ABCG2 and CXCR4 than adherent DU145 cells. (C) qRT-PCR: berbamine inhibited the expression of *ABCG2*, *CXCR4*, and *ALDH1A1* mRNA. DU145 CSCs expressed higher levels of *ABCG2* and *CXCR4* than the adherent DU145 cells. (D) Apoptosis assay: inhibition of ABCG2 and CXCR4 using the inhibitors Ko143 (1 μM) and WZ811 (5 μM) respectively, re-sensitized the CabaR-DU145 cells to cabazitaxel toxicity. Inhibition of ALDH1A1 using NCT-501 did not resensitize the CabaR-DU145 cells. Annexin V positive cells were considered apoptotic cells. The data were acquired from three separate experiments and calculated as means ± SD. $^{*}p < 0.05$, $^{**}p < 0.01$, $^{***}p < 0.001$, $^{****}p < 0.0001$. ns, not significant. [Color figure can be viewed at wileyonlinelibrary.com]

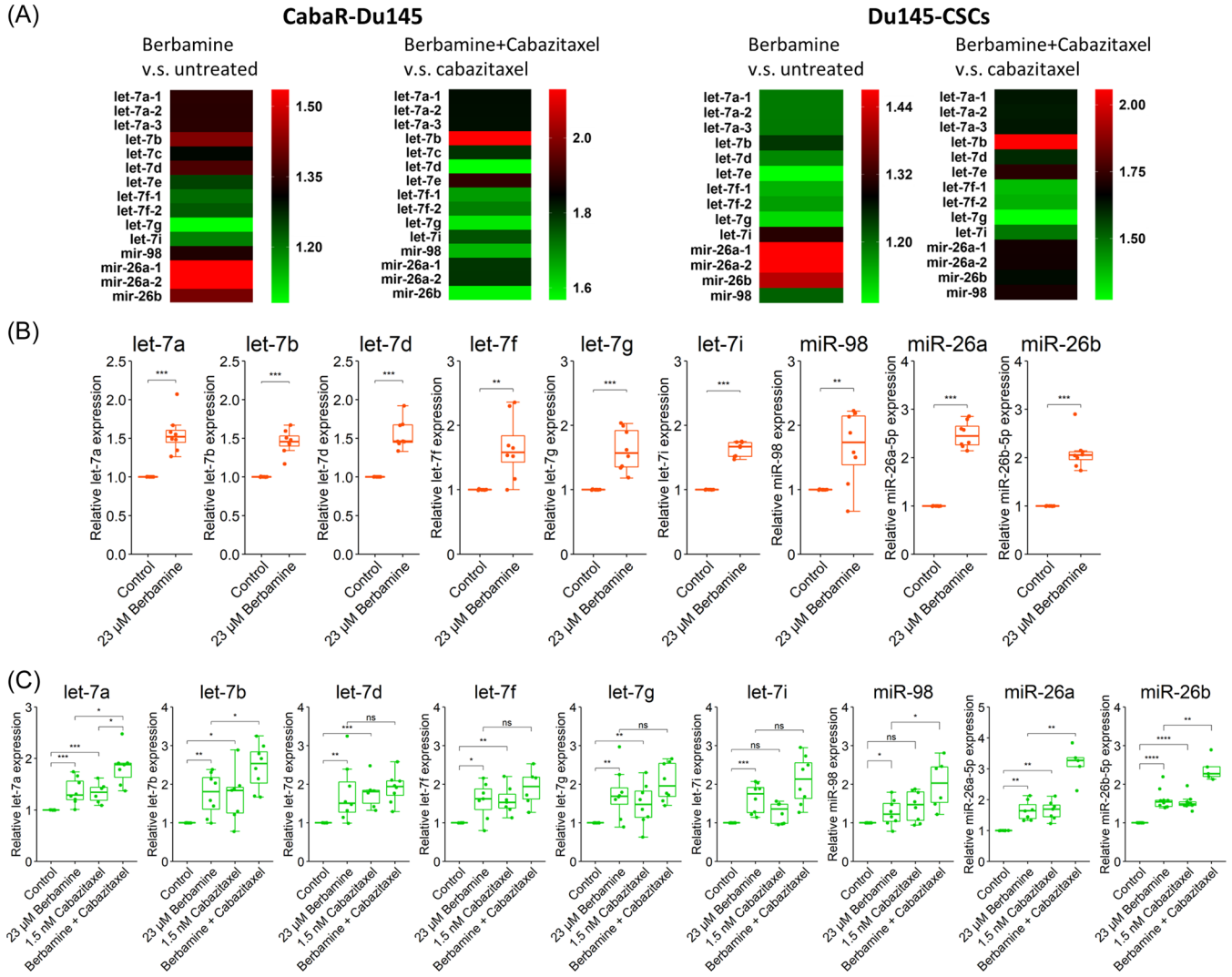

FIGURE 4 Berbamine resensitizes CabaR-DU145 cells to cabazitaxel via CXCR4/let-7/IGF2BP1 and ABCG2/miR-26b/p-STAT3 axes. (A) Heatmap of small RNA-sequencing results: berbamine enhanced the expression of the let-7 family members, miR-26a, and miR-26b in cabaR-DU145 cells and DU145 CSCs. Green represented 1, and red represented fold change of levels of miRNAs compared to 1. (B) Individual miRCURY LNA miRNA PCR assays: berbamine (23 μM) enhanced the expression of the let-7 family members, miR-26a, and miR-26b in CabaR-DU145 cells. (C) Individual miRCURY LNA miRNA PCR assays: berbamine enhanced the expression of let-7 family members, miR-26a, and miR-26b in DU145 CSCs. The combination of berbamine and cabazitaxel significantly upregulated the expression of the let-7 family members, miR-26a, and miR-26b. (D) qRT-PCR: berbamine downregulated the expression of *IGF2BP1* in DU145 CSCs. Also, silencing *CXCR4* using siRNAs downregulated the level of *IGF2BP1*. Control: untreated cells. Negative control: scrambled siRNA. (E) qRT-PCR: upregulation of let-7 family by mimics significantly suppressed the expression of *IGF2BP1*, both in CabaR-DU145 cells and DU145 CSCs. Control: untreated cells. Negative control: scrabbled siRNA. (F) qRT-PCR of DU145 CSCs: berbamine downregulated the expression of *STAT3*. Silencing *ABCG2* using siRNAs downregulated the expression of *STAT3*. (G) Flow cytometry of cabaR-DU145 cells: Berbamine and Ko143 (ABCG2 inhibitor) enhanced the expression of STAT3 while inhibiting the level of p-STAT3. (H) Flow cytometry of cabaR-DU145 cells: upregulation of miR-26b by mimics significantly suppressed the expression of p-STAT3 and enhanced the expression of STAT3. The combination of miR-26a mimics and miR-26b mimics also inhibited p-STAT3. The miR-26 inhibitor reversed the effect of the mimics. Control: untreated cells. Negative control: scrabbled siRNA. (I) Apoptosis assay using cabaR-DU145 cells: suppression of p-STAT3 and IGF2BP1 using the inhibitors Cryptotanshinone and BTYNB, respectively combined with cabazitaxel induced a higher apoptosis rate than cabazitaxel alone. The Annexin-positive cells were considered apoptotic cells. The data were acquired from three different experiments and calculated as means ± SEM. $^{*}p < 0.05$; $^{**}p < 0.01$; $^{***}p < 0.001$, $^{****}p < 0.0001$, ns, not significant. [Color figure can be viewed at wileyonlinelibrary.com]

suggested that berbamine might also influence the expression of let-7 and miR-26b via exosome delivery.

CabaR-DU145 cells obtained sensitivity to cabazitaxel when cocultured with exosomes derived from berbamine-treated CabaR-DU145 cells (Figure 5D,E). The results suggested that berbamine reversed the CabaR-DU145 resistance through enhancing the delivery of exosomal let-7, and miR-26b, as well as through the downregulation of IGF2BP1 and p-STAT3.

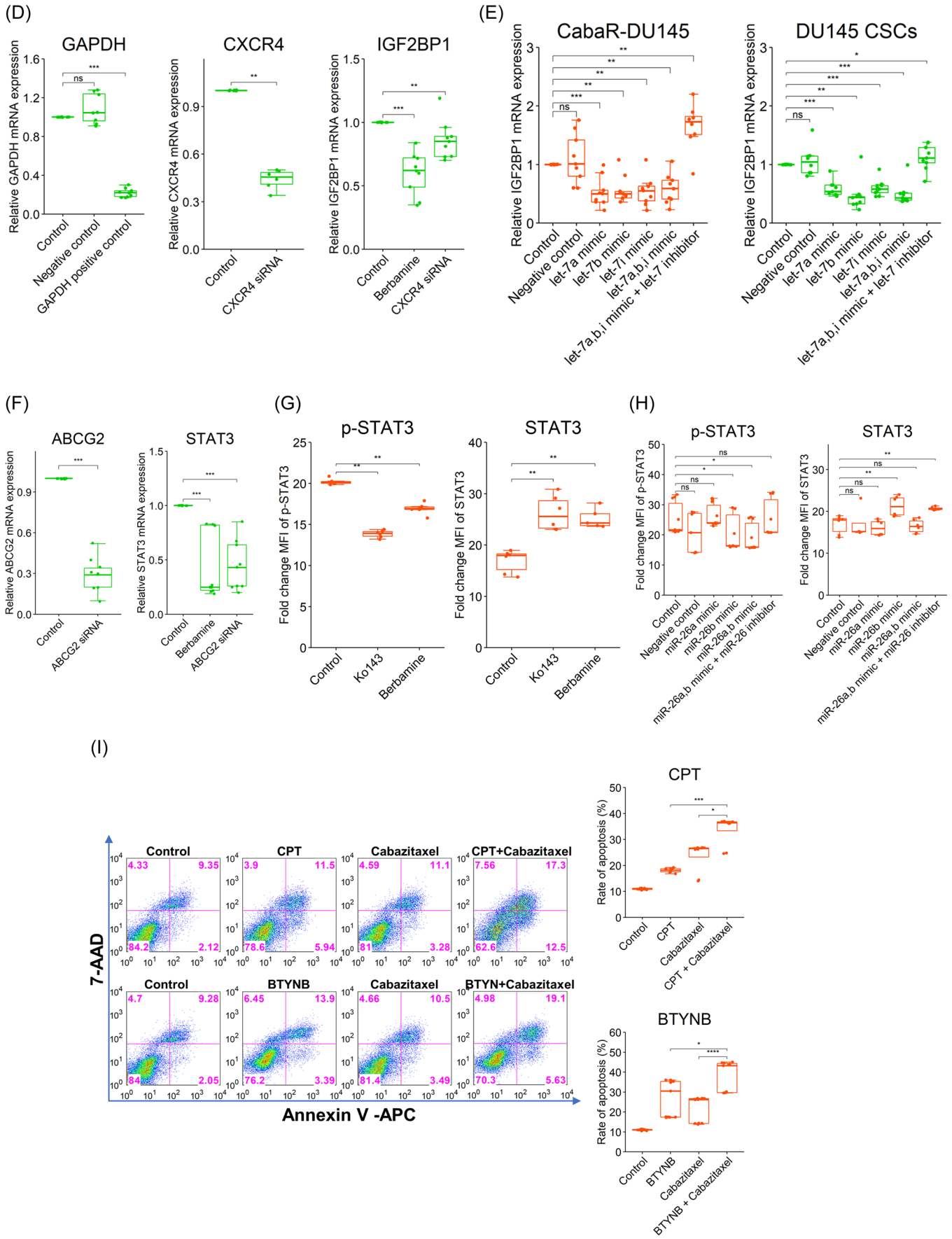

FIGURE 4 (Continued)

TABLE 1 The targets of let-7 miRNA family.

Gene symbol	Target score	Gene description
STARD13	100	StAR related lipid transfer domain containing 13
HMGA2	100	High mobility group AT-hook 2
IGDCC3	100	Immunoglobulin superfamily DCC subclass member 3
IGF2BP1	100	Insulin like growth factor 2 mRNA binding protein 1
FIGNL2	100	Fidgetin like 2
PRTG	100	Protogenin
NR6A1	100	Nuclear receptor subfamily 6 group A member 1
LIN28B	100	Lin-28 homolog B
ARID3B	100	AT-rich interaction domain 3B
C14orf28	100	Chromosome 14 open reading frame 28
TRIM71	100	Tripartite motif containing 71

4 | DISCUSSION

Prostate cancer is the most frequently diagnosed malignant disease, and the second cause of cancer death in men worldwide.[1] Importantly, unlike other types of cancers, PCa often relapses late, 5 years after prostatectomy, a tumor-free time period which is associated with "cure" in other cancer types.[28] PCa often develops resistance to antiandrogenic therapies and the chemotherapeutic agent cabazitaxel, which is the second-line chemotherapeutic drug after docetaxel fails in the treatment of advanced CRPC. The frequent development of drug resistance and PCa relapse highlight the critical medical need to find new agents that can reverse drug resistance. After a relapse, 90% of patients die within 15 years.[29] One reason for the late recurrence is so-called dormant disseminated tumor cells (DTCs) located in lymph nodes, bone, and the prostate bed. These cells are dormant and, therefore, mostly insensitive to treatment. Several extracellular molecules are described to maintain dormancy, like BMP-7 (bone morphogenetic protein 7) and WNT5A (Wnt Family Member 5A), whereas adrenergic signaling stimulates dormancy escape of DTCs in prostate cancer.[28] CSCs, discussed as a sub-population of DTCs, are undifferentiated cancer cells, responsible for tumor progression, invasion, tumor spread, and therapeutic relapse. They maintain self-renewal and stemness properties similar to other types of stem cells.[7,8] Several mechanisms are described that are related to the therapeutic resistance of CSCs, including cell cycle quiescence,[9] overexpression of efflux pumps like ABCG2 and detoxifying enzymes,[10,12,30,31] formation of the protective stem cell niche and DNA damage repair.[12]

Recently, studies reported that berbamine can target leukemia stem cells by suppressing phosphorylation of CaMKIIγ (Ca^{2+}/calmodulin-dependent protein kinase II-γ).[32] Our study now demonstrates that berbamine has an antitumor effect on both prostate cancer cells and prostate CSCs evidenced by assaying viability, proliferation, migration, invasion, and apoptosis, all cell characteristics responsible for drug resistance and recurrence.[33] Additionally, we found that berbamine enhanced the toxicity of cabazitaxel on both prostate cancer cells and prostate CSCs in the treatment combination berbamine plus cabazitaxel. Several CSC markers are connected to drug resistance or tumor relapse. ABCG2 is one of the CSC markers, belonging to the ABC transporter family, promoting cell resistance to drugs through drug efflux.[13,34] Inhibition of ABCG2 reverses multidrug resistance in several types of cancers like breast cancer,[35] hepatocellular cancer,[36] lung cancer,[37,38] and colorectal cancer.[39,40] Our results now demonstrate that berbamine reversed the cabazitaxel resistance by inhibition of ABCG2. CXCR4 is another marker often expressed on CSCs, which is related to tumor metastases and recurrence in prostate cancer.[15] Inhibition of CXCR4 re-sensitized prostate cancer cells to docetaxel,[16] colon cancer cells to paclitaxel,[41] chronic myelogenous leukemia cells to imatinib,[42] hepatocellular carcinoma cells to sorafenib,[43] blastoma cells to cisplatin,[44] lung cancer cells to cisplatin.[45] Our results demonstrated that berbamine re-sensitized cabazitaxel-resistant PCa cells to cabazitaxel via downregulating CXCR4.

It has been suggested that microRNAs can play a vital role in regulating CSCs. There is evidence that members of the let-7 family decrease the stemness of CSCs,[46] and target IGF2BP1 through 3' UTR regulation to influence the biological progress of carcinogenesis and drug resistance.[47,48] Within that scheme, miR-26b plays a role in cancer progression[49,50] through targeting downstream molecules.[51] MiR-26b enhances the sensitivity of doxorubicin,[51] cisplatin, temozolomide,[52] and maintains the CSC stemness properties.[53] Our results demonstrate further that berbamine targets prostate CSCs by regulating the CXCR4/let-7/IGF2BP1 axis and ABCG2/miR-26b/p-STAT3 axis. Future experiments would be conducted in vivo to investigate the pathways berbamine involved and to verify the antitumor effects on PCSCs in the mouse model.

Exosomes are small vesicles with a diameter of 40–100 nm, which can be secreted by tumor cells.[54] These vesicles carry proteins, mRNA, noncoding RNA, and DNA.[55] CSC-derived exosomes (CSC-EXO) are powerful tumor microenvironment mediators, maintaining tumor heterogeneity, changing tumor progression, and enhancing angiogenesis.[56] MicroRNAs can be delivered by exosomes and can influence downstream signaling pathways.[56] Our results demonstrate that berbamine enhanced the expression of exosomal let-7 miRNA family members, and miR-26b, implying that these miRNAs could be delivered through exosomes to facilitate intercellular communication, and further influence the expression of IGF2BP1 and p-STAT3. The observation that the treatment with exosomes derived from berbamine-treated CabaR-DU145 cells enhanced the sensitivity of CabaR-DU145 cells to cabazitaxel supports this hypothesis.

However, there are potential limitations that should be considered. On one hand, all the experiments were conducted with the AR negative cell lines, PC-3 and DU145, which represent a small population of prostate cancer. In our following experiments, the AR-positive cell line like LNCaP will be included. On the other hand, the results should be tested in vivo using mouse models to further illustrate the antitumor effect of berbamine on PCSCs.

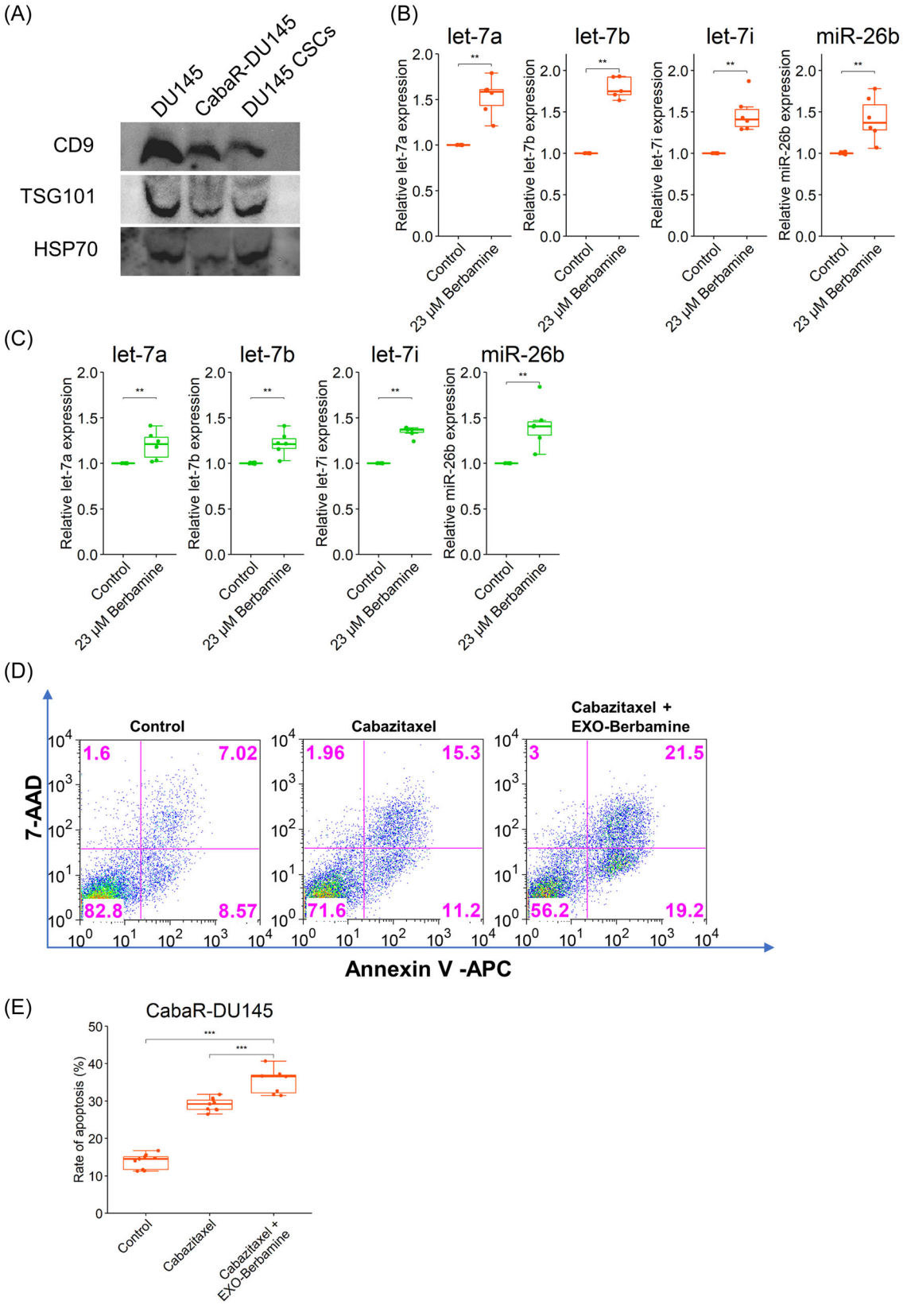

FIGURE 5 (See caption on next page).

5 | CONCLUSIONS

Our results document for the first time that berbamine enhances the antitumor effect of cabazitaxel on PCSCs and inhibits the expression of the CSC markers of ABCG2, CXCR4, and ALDH1A1. Inhibition of ABCG2 and CXCR4 can resensitize CabaR-DU145 cells to cabazitaxel. Furthermore, both berbamine treatment and downregulation of CXCR4 enhanced members of the let-7 family, and downregulated the target IGF2BP1. In addition to the downregulation of ABCG2, berbamine enhanced the expression of miR-26b, and thereby inhibited the target p-STAT3. Inhibition of IGF2BP1 and p-STAT3 re-sensitized the CabaR-DU145 cells to cabazitaxel. Finally, berbamine enhanced the expression of exosomal let-7a, let-7b, let-7i, miR-26b, which implies that berbamine can also influences the biological activities of CSCs through exosome delivery. Importantly, exosomes derived from berbamine-treated CabaR-DU145 cells induced more apoptosis. The suggested mode of action is summarized in Figure 6. It is highlighted that berbamine targets the prostate cancer cells and CSCs, and reverses the cabazitaxel resistance

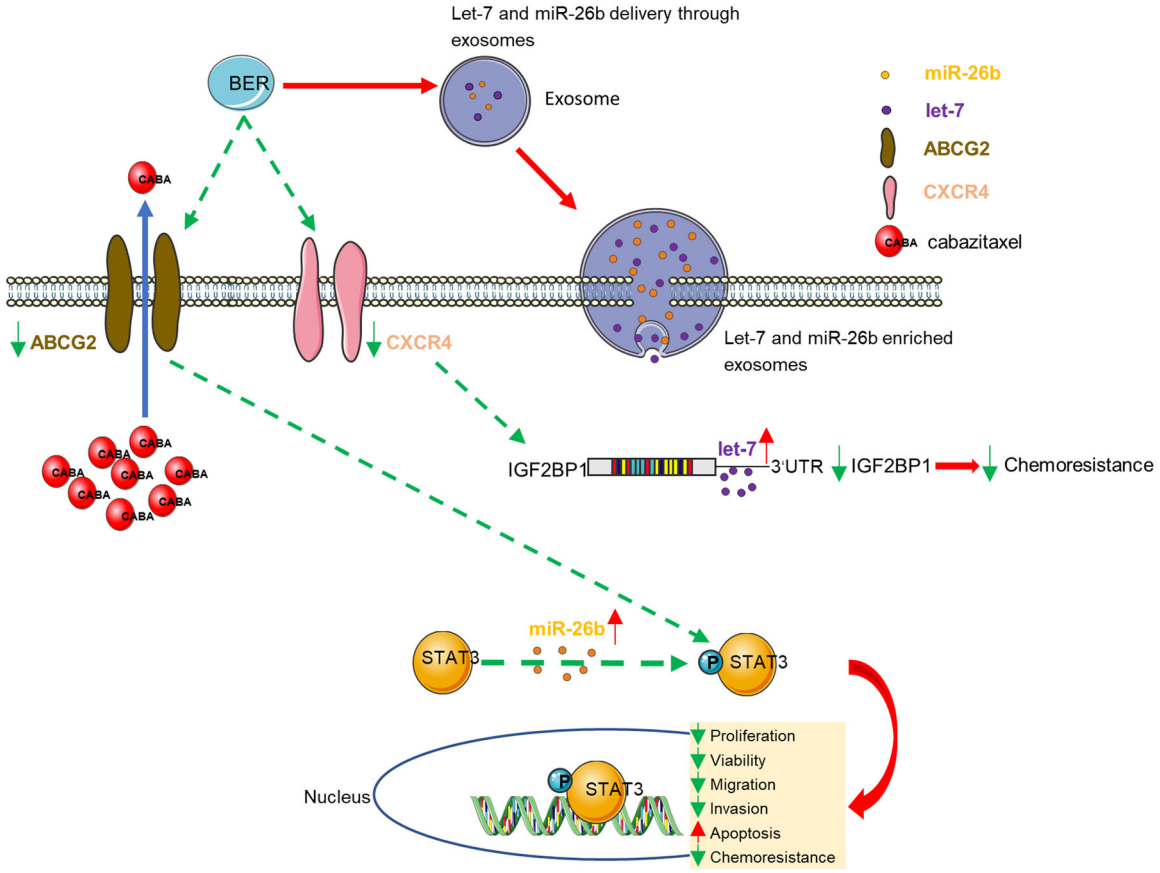

FIGURE 6 Suggested mechanisms of berbamine effects in antitumor activity and reversal of cabazitaxel resistance. Berbamine inhibits the efflux pump ABCG2 thereby increasing the concentration of cabazitaxel in tumor cells. Berbamine, additionally, enhances antitumor activity and drug sensitivity through the CXCR4/let-7 miRNA/IGF2BP1 and ABCG2/miR-26b/p-STAT3 axes by enhancing the expression of the let-7 miRNA family members, and miR-26b, which decrease the activation or expression of IGF2BP1 and p-STAT3, respectively. Downregulation of IGF2BP1 and p-STAT3 could reverse cabazitaxel resistance. The let-7 and miR-26b can be delivered by exosomes evidenced by enhanced presence of exosomal let-7 family members and miR-26b after berbamine treatment. Furthermore, inhibition of ABCG2 downregulates the p-STAT3 expression, and inhibition of CXCR4 can downregulate the IGF2BP1 expression. BER, berbamine; green and dotted line, decreasing effects; red line, increasing effects. [Color figure can be viewed at wileyonlinelibrary.com]

FIGURE 5 Exosomal miRNAs of the let-7 family and miR-26b-5p induce apoptosis. (A) Western blot: exosomes were extracted from the supernatants of DU145, cabaR-DU145 cells, and DU145 CSCs using the ExoQuick-TC kit. The exosomal markers CD9, TSG101, and HSP70 were detected according to their molecular weight after staining with the specific antibodies. (B and C) Exosomes were extracted from the cell culture supernatant of CabaR-DU145 cells and DU145 CSCs with or without treatment of berbamine (23 μM) for 4 days using miRCURY® Exosome Cell/Urine/CSF Kit. After extracting the total RNAs from exosomes using the miRNeasy Micro kit, cDNA synthesis, and miRCURY LNA miRNA PCR assay was performed: berbamine enhanced the expression of exosomal let-7a, let-7b, let-7i, and miR-26b both in CabaR-DU145 cells (B) and DU145 CSCs (C). (D and E) Apoptosis assay: CabaR-DU145 cells showed a higher apoptosis rate when they were cultured with exosomes derived from berbamine-treated CabaR-DU145 cells compared to cabazitaxel alone. The data were acquired from three different experiments and calculated as means ± SD. $^{*}p < 0.05$; $^{**}p < 0.01$; $^{***}p < 0.001$. $^{****}p < 0.0001$. [Color figure can be viewed at wileyonlinelibrary.com]

through the CXCR4/let-7//IGF2BP1 axis and the ABCG2/miR-26b/p-STAT3 axis.

AUTHOR CONTRIBUTIONS

Lili Wang: Data curation; formal analysis; investigation; methodology; resources; software; validation; visualization; writing—original draft preparation. **Chen Lyu**: Methodology; resources; writing—review & editing. **Birgit Stadlbauer**: Methodology; resources; software; writing—review & editing. **Alexander Buchner**: Methodology; software, supervision; writing—review & editing. **Elfriede Nößner**: Supervision; writing—review & editing. **Heike Pohla**: Conceptualization; funding acquisition; investigation; methodology; project administration; resources; software; supervision; validation; writing—review & editing. All authors have read and agreed to the published version of the manuscript.

ACKNOWLEDGMENTS

The author Lili Wang was funded by the China scholarship council, grant number 201706270196. Open Access funding enabled and organized by Projekt DEAL.

CONFLICT OF INTEREST STATEMENT

The authors declare no conflict of interest.

DATA AVAILABILITY STATEMENT

The data that support the findings of this study are available from the corresponding author upon reasonable request.

ORCID

Heike Pohla http://orcid.org/0000-0001-8296-2059

REFERENCES

1. Sung H, Ferlay J, Siegel RL, et al. Global cancer statistics 2020: GLOBOCAN estimates of incidence and mortality worldwide for 36 cancers in 185 countries. *CA Cancer J Clin*. 2021;71:209-249.
2. Kahn B, Collazo J, Kyprianou N. Androgen receptor as a driver of therapeutic resistance in advanced prostate cancer. *Int J Biol Sci*. 2014;10:588-595.
3. Amaral TMS, Macedo D, Fernandes I, Costa L. Castration-resistant prostate cancer: mechanisms, targets, and treatment. *Prostate Cancer*. 2012;2012:1-11.
4. Tucci M, Caffo O, Buttigliero C, et al. Therapeutic options for first-line metastatic castration-resistant prostate cancer: suggestions for clinical practise in the CHAARTED and LATITUDE era. *Cancer Treat Rev*. 2019;74:35-42.
5. Feldman BJ, Feldman D. The development of androgen-independent prostate cancer. *Nat Rev Cancer*. 2001;1:34-45.
6. Moreira DM, Howard LE, Sourbeer KN, et al. Predictors of time to metastasis in castration-resistant prostate cancer. *Urology*. 2016;96:171-176.
7. Kreso A, Dick JE. Evolution of the cancer stem cell model. *Cell Stem Cell*. 2014;14:275-291.
8. Lobo NA, Shimono Y, Qian D, Clarke MF. The biology of cancer stem cells. *Annu Rev Cell Dev Biol*. 2007;23:675-699.
9. Borst P. Cancer drug pan-resistance: pumps, cancer stem cells, quiescence, epithelial to mesenchymal transition, blocked cell death pathways, persisters or what? *Open Biol*. 2012;2:120066.
10. Bunting KD. ABC transporters as phenotypic markers and functional regulators of stem cells. *Stem Cells*. 2002;20:11-20.
11. Sugano T, Seike M, Noro R, et al. Inhibition of ABCB1 overcomes cancer stem cell-like properties and acquired resistance to MET inhibitors in non-small cell lung cancer. *Mol Cancer Ther*. 2015;14:2433-2440.
12. Hong M, Tan HY, Li S, et al. Cancer stem cells: the potential targets of Chinese medicines and their active compounds. *Int J Mol Sci*. 2016;17:893.
13. Harris KS, Kerr BA. Prostate cancer stem cell markers drive progression, therapeutic resistance, and bone metastasis. *Stem Cells Int*. 2017;2017:1-9.
14. Leonard GD, Fojo T, Bates SE. The role of ABC transporters in clinical practice. *Oncologist*. 2003;8:411-424.
15. Mochizuki H, Matsubara A, Teishima J, et al. Interaction of ligand-receptor system between stromal-cell-derived factor-1 and CXC chemokine receptor 4 in human prostate cancer: a possible predictor of metastasis. *Biochem Biophys Res Commun*. 2004;320:656-663.
16. Domanska UM, Timmer-Bosscha H, Nagengast WB, et al. CXCR4 inhibition with AMD3100 sensitizes prostate cancer to docetaxel chemotherapy. *Neoplasia*. 2012;14:709-718.
17. Li T, Su Y, Mei Y, et al. ALDH1A1 is a marker for malignant prostate stem cells and predictor of prostate cancer patients' outcome. *Lab Invest*. 2010;90:234-244.
18. Germann M, Wetterwald A, Guzmán-Ramirez N, et al. Stem-like cells with luminal progenitor phenotype survive castration in human prostate cancer. *Stem Cells*. 2012;30:1076-1086.
19. Zhao Y, Tan Y, Wu G, et al. Berbamine overcomes imatinib-induced neutropenia and permits cytogenetic responses in Chinese patients with chronic-phase chronic myeloid leukemia. *Int J Hematol*. 2011;94:156-162.
20. Wang S, Liu Q, Zhang Y, et al. Suppression of growth, migration and invasion of highly-metastatic human breast cancer cells by berbamine and its molecular mechanisms of action. *Mol Cancer*. 2009;8:81.
21. Nam S, Xie J, Perkins A, et al. Novel synthetic derivatives of the natural product berbamine inhibit Jak2/Stat3 signaling and induce apoptosis of human melanoma cells. *Mol Oncol*. 2012;6:484-493.
22. Yang F, Nam S, Brown CE, et al. A novel berbamine derivative inhibits cell viability and induces apoptosis in cancer stem-like cells of human glioblastoma, via up-regulation of miRNA-4284 and JNK/AP-1 signaling. *PLoS One*. 2014;9:e94443.
23. Al-Mansouri L, Gurney H. Clinical concepts for cabazitaxel in the management of metastatic castration-resistant prostate cancer. *Asia Pac J Clin Oncol*. 2019;15:288-295.
24. Schindelin J, Arganda-Carreras I, Frise E, et al. Fiji: an open-source platform for biological-image analysis. *Nat Methods*. 2012;9:676-682.
25. Pontén F, Jirström K, Uhlen M. The Human Protein Atlas— a tool for pathology. *J Pathol*. 2008;216:387-393.
26. Chandrashekar DS, Karthikeyan SK, Korla PK, et al. UALCAN: an update to the integrated cancer data analysis platform. *Neoplasia*. 2022;25:18-27.
27. Wang L, Stadlbauer B, Lyu C, Buchner A, Pohla H. Shikonin enhances the antitumor effect of cabazitaxel in prostate cancer stem cells and reverses cabazitaxel resistance by inhibiting ABCG2 and ALDH3A1. *Am J Cancer Res*. 2020;10:3784-3800.
28. Cackowski FC, Heath EI. Prostate cancer dormancy and recurrence. *Cancer Lett*. 2022;524:103-108.
29. Freedland SJ, Humphreys EB, Mangold LA, et al. Death in patients with recurrent prostate cancer after radical prostatectomy: prostate-specific antigen doubling time subgroups and their associated contributions to all-cause mortality. *J Clin Oncol*. 2007;25:1765-1771.
30. Steinbichler TB, Dudás J, Skvortsov S, Ganswindt U, Riechelmann H, Skvortsova II. Therapy resistance mediated by cancer stem cells. *Sem Cancer Biol*. 2018;53:156-167.

31. Begicevic RR, Falasca M. ABC transporters in cancer stem cells: beyond chemoresistance. *Int J Mol Sci*. 2017;18:2362.
32. Gu Y, Chen T, Meng Z, et al. CaMKII γ, a critical regulator of CML stem/progenitor cells, is a target of the natural product berbamine. *Blood*. 2012;120:4829-4839.
33. Zhou HM, Zhang JG, Zhang X, Li Q. Targeting cancer stem cells for reversing therapy resistance: mechanism, signaling, and prospective agents. *Signal Transduct Target Ther*. 2021;6:62.
34. Patrawala L, Calhoun T, Schneider-Broussard R, Zhou J, Claypool K, Tang DG. Side population is enriched in tumorigenic, stem-like cancer cells, whereas ABCG2+ and ABCG2- cancer cells are similarly tumorigenic. *Cancer Res*. 2005;65:6207-6219.
35. Ni W, Fan H, Zheng X, et al. Cryptotanshinone inhibits ERα-dependent and -independent BCRP oligomer formation to reverse multidrug resistance in breast cancer. *Front Oncol*. 2021;11:624811.
36. Liang X, Wang Y, Shi H, Dong M, Han H, Li Q. Nucleolin-targeting AS1411 aptamer-modified micelle for the co-delivery of doxorubicin and miR-519c to improve the therapeutic efficacy in hepatocellular carcinoma treatment. *Int J Nanomedicine*. 2021;16:2569-2584.
37. Lei ZN, Teng QX, Gupta P, et al. Cabozantinib reverses topotecan resistance in human non-small cell lung cancer NCI-H460/TPT10 cell line and tumor xenograft model. *Front Cell Dev Biol*. 2021;9:640957.
38. Wu ZX, Yang Y, Wang G, et al. Dual TTK/CLK2 inhibitor, CC-671, selectively antagonizes ABCG2-mediated multidrug resistance in lung cancer cells. *Cancer Sci*. 2020;111:2872-2882.
39. Narayanan S, Gujarati NA, Wang JQ, et al. The novel benzamide derivative, VKNG-2, restores the efficacy of chemotherapeutic drugs in colon cancer cell lines by inhibiting the ABCG2 transporter. *Int J Mol Sci*. 2021;22:2463.
40. Wang Z, Zhan Y, Xu J, et al. β-sitosterol reverses multidrug resistance via BCRP suppression by inhibiting the p53–MDM2 interaction in colorectal cancer. *J Agricult Food Chem*. 2020;68:3850-3858.
41. Nengroo MA, Maheshwari S, Singh A, et al. CXCR4 intracellular protein promotes drug resistance and tumorigenic potential by inversely regulating the expression of death receptor 5. *Cell Death Dis*. 2021;12:464.
42. Cao H, Gao Y, Wang R, Guo Q, Hui H. Wogonin reverses the drug resistance of chronic myelogenous leukemia cells to imatinib through CXCL12-CXCR4/7 axis in bone marrow microenvironment. *Ann Transl Med*. 2020;8:1046.
43. Zheng N, Liu W, Li B, et al. Co-delivery of sorafenib and metapristone encapsulated by CXCR4-targeted PLGA-PEG nanoparticles overcomes hepatocellular carcinoma resistance to sorafenib. *J Exp Clin Cancer Res*. 2019;38:232.
44. Li C, Yang C, Wei G. Vandetanib inhibits cisplatinresistant neuroblastoma tumor growth and invasion. *Oncol Rep*. 2018;39:1757-1764.
45. Xie S, Tu Z, Xiong J, et al. CXCR4 promotes cisplatin-resistance of non-small cell lung cancer in a CYP1B1-dependent manner. *Oncol Rep*. 2017;37:921-928.
46. Chirshev E, Hojo N, Bertucci A, et al. Epithelial/mesenchymal heterogeneity of high-grade serous ovarian carcinoma samples correlates with miRNA let-7 levels and predicts tumor growth and metastasis. *Mol Oncol*. 2020;14:2796-2813.
47. Busch B, Bley N, Müller S, et al. The oncogenic triangle of HMGA2, LIN28B and IGF2BP1 antagonizes tumor-suppressive actions of the let-7 family. *Nucleic Acids Res*. 2016;44:3845-3864.
48. Huang X, Zhang H, Guo X, Zhu Z, Cai H, Kong X. Insulin-like growth factor 2 mRNA-binding protein 1 (IGF2BP1) in cancer. *J Hematol Oncol*. 2018;11:88.
49. Zhang C, Tong J, Huang G. Nicotinamide phosphoribosyl transferase (Nampt) is a target of microRNA-26b in colorectal cancer cells. *PLoS One*. 2013;8:e69963.
50. Xia M, Duan ML, Tong JH, Xu JG. MiR-26b suppresses tumor cell proliferation, migration and invasion by directly targeting COX-2 in lung cancer. *Eur Rev Med Pharmacol Sci*. 2015;19:4728-4737.
51. Chen E, Li E, Liu H, et al. miR-26b enhances the sensitivity of hepatocellular carcinoma to Doxorubicin via USP9X-dependent degradation of p53 and regulation of autophagy. *Int J Biol Sci*. 2021;17:781-795.
52. Wang L, Su J, Zhao Z, et al. MiR-26b reverses temozolomide resistance via targeting Wee1 in glioma cells. *Cell Cycle*. 2017;16:1954-1964.
53. Khosla R, Hemati H, Rastogi A, Ramakrishna G, Sarin SK, Trehanpati N. miR-26b-5p helps in EpCAM+cancer stem cells maintenance via HSC71/HSPA8 and augments malignant features in HCC. *Liver Int*. 2019;39:1692-1703.
54. Heiler S, Wang Z, Zöller M. Pancreatic cancer stem cell markers and exosomes—the incentive push. *World J Gastroenterol*. 2016;22:5971-6007.
55. Vlassov AV, Magdaleno S, Setterquist R, Conrad R. Exosomes: current knowledge of their composition, biological functions, and diagnostic and therapeutic potentials. *Biochim Biophys Acta Gen Subj*. 2012;1820:940-948.
56. Sharma A. Role of stem cell derived exosomes in tumor biology. *Int J Cancer*. 2018;142:1086-1092.

SUPPORTING INFORMATION

Additional supporting information can be found online in the Supporting Information section at the end of this article.

How to cite this article: Wang L, Lyu C, Stadlbauer B, Buchner A, Nößner E, Pohla H. Berbamine targets cancer stem cells and reverses cabazitaxel resistance via inhibiting IGF2BP1 and p-STAT3 in prostate cancer. *The Prostate*. 2024;84:131-147. doi:10.1002/pros.24632